Colloid and Polymer Science (2021) 299:1447–1458
https://doi.org/10.1007/s00396-021-04869-8

ORIGINAL CONTRIBUTION

Crystallization, rheological and mechanical properties of poly(butylene succinate)/poly(propylene carbonate)/poly(vinyl acetate) ternary blends

Han Xu[1] · Yancun Yu[2] · Yi Li[2]

Received: 20 May 2021 / Revised: 8 July 2021 / Accepted: 12 July 2021 / Published online: 19 July 2021

Abstract
Herein, a ternary blend from poly(butylene succinate) (PBS), poly(propylene carbonate) (PPC), and poly(vinyl acetate) (PVAc) with improved crystallization rate, stiffness, and toughness was initially prepared via melt compounded. The influence of PVAc content on morphology, miscibility, thermal behavior, and rheological and mechanical properties was investigated. Scanning electron microscopy observation showed phase morphology of PBS/PPC/PVAc ternary blends evolved from sea-island dispersion to co-continuous structure. Dynamic mechanical analysis revealed that PBS and PPC were immiscible. The presence of PPC inhibited the crystallization of PBS, while simultaneous incorporation of PVAc and PPC promoted the crystallization. Furthermore, the introduction of PPC and PVAc enhanced the rheological properties of PBS. Unexpectedly, prominent improvement in tensile modulus, yield strength, and elongation was obtained for the PBS/PPC/PVAc ternary blend with 10 wt% PVAc due to the morphological evolution from sea-island to co-continuous structure, which was respectively increased by 93%, 52%, and 26% compared with neat PBS.

Keywords Poly(butylene succinate) · Poly(propylene carbonate) · Poly(vinyl acetate) · Blends · Crystallization

Introduction

The increasing concerns regarding renewable resource-derived and biodegradable plastics have exerted a lot of research because the traditional petroleum-based plastics consume limited petroleum resources and are difficult to degrade in the environment [1]. Poly(butylene succinate) (PBS), as a biodegradable environmentally friendly polyester, has attracted much attention due to its potential to replace petroleum-based polymer in commodity applications [2, 3]. In the past, the monomers for polycondensation to synthesize PBS, namely succinic acid and 1,4-butanediol, could only be derived from fossil raw materials. However currently, the monomers can also be obtained from non-fossil renewable natural resources [4]. PBS is a thermoplastic aliphatic semi-crystalline polymer with high chemical and thermal resistance, good elongation, excellent melt processability, and low cost [5]. The other physical properties of PBS are similar to those of polypropylene and polyethylene. However, neat PBS shows low mechanical strength, modulus, and melt strength. These inherent drawbacks of PBS have greatly limited its large-scale commercial applications [6].

Poly(propylene carbonate) (PPC), another widely studied biodegradable biopolymer, is synthesized by polycondensation of carbon dioxide (CO_2) and propylene oxide with zinc glutarate as catalyst [7]. It is amorphous and has good processability so that it can be molded by various thermoplastic processing methods. However, the poor mechanical properties and low glass transition temperature and decomposition temperature of PPC have become a bottleneck for its further development and application [8].

It can be seen that an individual biomass polymer may not meet high performance requirements of practical applications. To improve and tailor the performance of biopolymers and further expand their applications, several processing techniques, such as copolymerization, physical

✉ Yancun Yu
yuyc@ciac.ac.cn

[1] School of Materials Science and Engineering, Harbin Institute of Technology, Weihai 264209, China

[2] Key Laboratory of Polymer Ecomaterials, Changchun Institute of Applied Chemistry, Chinese Academy of Sciences, Changchun 130022, China

blending, and reinforcement with fillers have been extensively studied. Among them, blending with other biodegradable polymers is a very effective and environmentally friendly modification method. So far, many biodegradable polymers, including poly(lactic acid) (PLA) [9–11], poly(ε-caprolactone) (PCL) [12, 13], poly(ethylene oxide) (PEO) [14, 15], poly(hydroxybutyrate) (PHB) [16], and poly(vinyl phenol) (PVP) [17], have been used to blend with PBS to prepare binary blends with improved properties. Binary blends composed of PBS and PPC were also fabricated in order to obtain the desirable mechanical features [18–20]. The introduction of 10 wt% PBS into PPC increased the tensile strength of PPC by 60%, but the elongation at break would decrease by 24% [18]. The crystallization temperature of PBS was increased by the incorporation of PPC, while the thermal stability of PBS was greatly decreased [19]. It can be seen that the major disadvantage of binary blends is that one property is greatly reduced when other properties are improved.

Compared to binary blends, ternary blends show a better balance of properties. However, there have been few investigations on the ternary blends containing sustainable PPC and biodegradable PBS. Therefore, in the present work, we used poly(vinyl acetate) (PVAc) as the third phase to fabricate a PBS/PPC/PVAc ternary blend system. PVAc is amorphous and has high melt viscosity. It is notable that PVAc can be melt-mixed with some biodegradable polymers to prepare partially miscible or full miscible blend systems to improve the mechanical properties of biodegradable polymers [21–25]. It was found in our previous studies that the incorporation of PVAc into PBS improved the mechanical properties and accelerated the crystallization rate of PBS matrix [25]. Considering the amorphous nature of both PPC and PVAc, as well as the compatibility between PBS, PPC, and PVAc, the focus of this work is to prepare PBS/PPC/PVAc ternary blends with excellent balance performance by melt blending method. The content of the third phase PVAc on the miscibility, phase morphology, crystallization behavior, and rheological and mechanical properties of PBS/PPC binary blends was systematically investigated.

Experimental

Materials

PBS was supplied by Xinjiang Blue Ridge Tunhe Chemical Industry Joint Stock Co., Ltd. and had a weight-average molecular weight (M_w) of 1.7×10^5 g mol^{-1} and a polydispersity of 1.82. PPC with an M_w of 10^5 g mol^{-1} and polydispersity of 2.60 was synthesized by the copolymerization between carbon dioxide and epoxy propane. PVAc used in this work was purchased from Nuoda New Materials Company. It had M_w and polydispersity of 1.5×10^5 g mol^{-1} and 1.54, respectively.

Sample preparation

PBS, PPC, and PVAc pellets were dried in vacuum for 10 h before melt blending, and the drying temperatures were 70, 50, and 50 °C, respectively. The PBS/PPC binary and PBS/PPC/PVAc ternary blends were fabricated in a Haake batch intensive mixer (Haake Rheomix 600, Karlsruhe, Germany). The mixing was performed at a speed of 50 rpm and a temperature of 150 °C for 7 min. The mixture was melted at 160 °C for about 5 min, then melt-pressed at 10 MPa for 2 min to form a sheet with a thickness of 1 mm, followed by cold-pressed and shaped at room temperature. The weight ratio of PBS/PPC in the ternary blends was kept fixed at 70/30. The weight fractions of PVAc in the ternary blends were changed from 5 to 20 wt% on the basis of total PBS/PPC blend weight. For convenience, the PBS/PPC/PVAc blends were labeled as PBS/PPC-X, where X was the weight content of PVAc in the ternary blends.

Characterization

Scanning electronic microscopy

SEM (FEI Co., Eindhoven, Netherlands) was used to observe the phase morphology of PBS/PPC binary and PBS/PPC/PVAc ternary blends. The acceleration voltage was set at 10 kV. In order to prevent the deformation of the imaging surface, the samples were fractured cryogenically. Then the PPC minor phase was etched in acetone solution for 120 min at room temperature. Before SEM observation, the etched surfaces were sputter coated with a thin layer of gold to improve the electrical conductivity of samples.

Dynamic mechanical analysis

DMA was carried out by using a DMA Q800 from TA Instruments (USA) in a tensile mode with a frequency of 1 Hz. The dimension of rectangle samples was $20\times10\times1.0$ mm^3. The temperature was swept from − 60 to 100 °C at a rate of 3 °C min^{-1}.

Differential scanning calorimetry

Thermal and crystallization behaviors of PBS/PPC binary and PBS/PPC/PVAc ternary blends were studied with a TA Instrument DSC Q20 (USA) under nitrogen atmosphere. First, each sample of 5 − 8 mg was heated from 0 to 150 °C at a heating rate of 100 °C min^{-1}, and maintained at 150 °C for 3 min. Then, the molten sample was cooled to 0 °C at a cooling rate of 10 °C min^{-1} (first cooling). The

crystallization temperature (T_c) and crystallization enthalpy (ΔH_c) were obtained from the first cooling DSC scans. After that, the samples were heated to 150 °C again at a rate of 10 °C min^{-1} (second heating). The melting temperature (T_m) and melting enthalpy (ΔH_m) were obtained from the second heating DSC scans. ΔH_c and ΔH_m had been corrected on the basis of the weight content of PBS in the blends. The degree of crystallinity of PBS matrix (X_c) in the blends was estimated by using the following formula:

$$X_c = \frac{\Delta H_c}{\Delta H_m^0 a} \times 100\% \bullet X_c \quad (1)$$

where ΔH_m^0 is the melting enthalpy when X_c of PBS is 100%, taking the value of 110.3 J g^{-1} [26], and α is the weight percentage of PBS in the blends.

Rheological measurements

Rheological tests of all samples were carried out on a rotational rheometer (TA Series AR2000ex, TA Instrument, USA). The diameter of the parallel plate of the rheometer was 25 mm, and the thickness of the sample was about 1 mm. The dynamic frequency sweep was performed at 150 °C from 0.05 to 100 rad s^{-1}. The strain value was fixed at 1.25% in order to keep the response of the samples within the linear viscoelastic range.

Tensile tests

Tensile measurements were conducted on tensile testing machine (Instron-1121, USA) at ambient temperature with a fixed crosshead speed of 50 mm min^{-1} on the basis of ISO 527–1:2012 standard. Specimens (20 × 4 × 1 mm^3) were cut from the previously compression-molded sheets into a dumbbell shape. The value of each mechanical property is the average of five repetitions.

Results and discussion

Phase morphology of the blends

The physical and mechanical properties of multiphase polymer blends are affected by phase morphology, so that studying the phase morphology of blends is of great significance for establishing the relationship between performance and morphology. The SEM micrographs of PBS/PPC binary and PBS/PPC/PVAc ternary are shown in Fig. 1. The morphology of PPC domain in these blends was represented by black pores (PPC removed). As can be seen from Fig. 1a, b, the PBS/PPC binary blend presented a typical sea-island morphology, suggesting the immiscibility between PBS matrix and dispersed PPC phase. Moreover, the PPC in the PBS/PPC binary blend was uniformly dispersed in the PBS matrix as small droplets with a size from 5.26 to 0.78 μm and an average size of 2.87 μm. As well known, the morphology of blends depends on the competing between coalescence and breakup of droplets. Although under the high shear field of the mixing, the droplet breakup is the main effect, both droplet breakup and coalescence occur. According to the applied shear rate and the surface energy of interface, there will be a kind of establishment between droplet breakup and coalescence [27]. As seen in Fig. 1c, d, the PBS/PPC/PVAc ternary blend with 5 wt% PVAc showed finer dispersed structure and smaller droplets with sizes varying from 4.54 to 1.01 μm and an average size of 2.10 μm, which clearly indicated a dominance of droplet breakup. This may be attributed to the fact that the introduction of PVAc into the PBS/PPC binary blend reduced the interface energy between PBS and PPC. As the PVAc concentration was increased to 10 wt% (Fig. 1e, f), the morphology of PBS/PPC/PVAc ternary blend transitioned from sea-island structure to co-continuous structure. When the PVAc concentration was increased to 20 wt%, co-continuous structure became coarser (Fig. 1g, h). This observation implied that PVAc with high content and PPC together form a co-continuous structure.

Phase miscibility of the blends

DMA tests were employed to examine the mutual miscibility of PVAc with PBS and PPC components in PBS/PPC/PVAc ternary systems. This is due to the fact that the phase morphology depended on the interfacial interaction and compatibility between the components. The damping factor (tan δ) and storage modulus (G') curves of neat PBS, PPC, and PVAc as well as PBS/PPC binary and PBS/PPC/PVAc ternary blends are shown in Fig. 2a, b, respectively. The tan δ is associated with the glass transition of polymer, whereas the storage modulus can directly reflect the elastic response of polymer when subjected to shearing force.

The values of T_g of all samples can be obtained from the peaks of tan δ curves and are summarized in Table 1. As can be seen from Fig. 2a and Table 1, neat PBS, PPC, and PVAc exhibited single transitions at − 19.0, 34.5, and 45.8 °C, respectively. For PBS/PPC binary blend, two transitions were visible in the tan δ curve. The transitions which appeared at − 20.9 and 37.8 °C for PBS/PPC binary blend were related to the PBS matrix and PPC phase, respectively. Compared with neat PBS and PPC, the T_gs of PBS and PPC in the PBS/PPC binary blend moved away from each other, indicating that PBS and PPC were totally immiscible, which was consistent with the results observed by Pang et al. [19]. Noteworthily, a reduction in the T_g of PBS and an increase in the T_g of PPC in PBS/PPC binary blend were observed. The

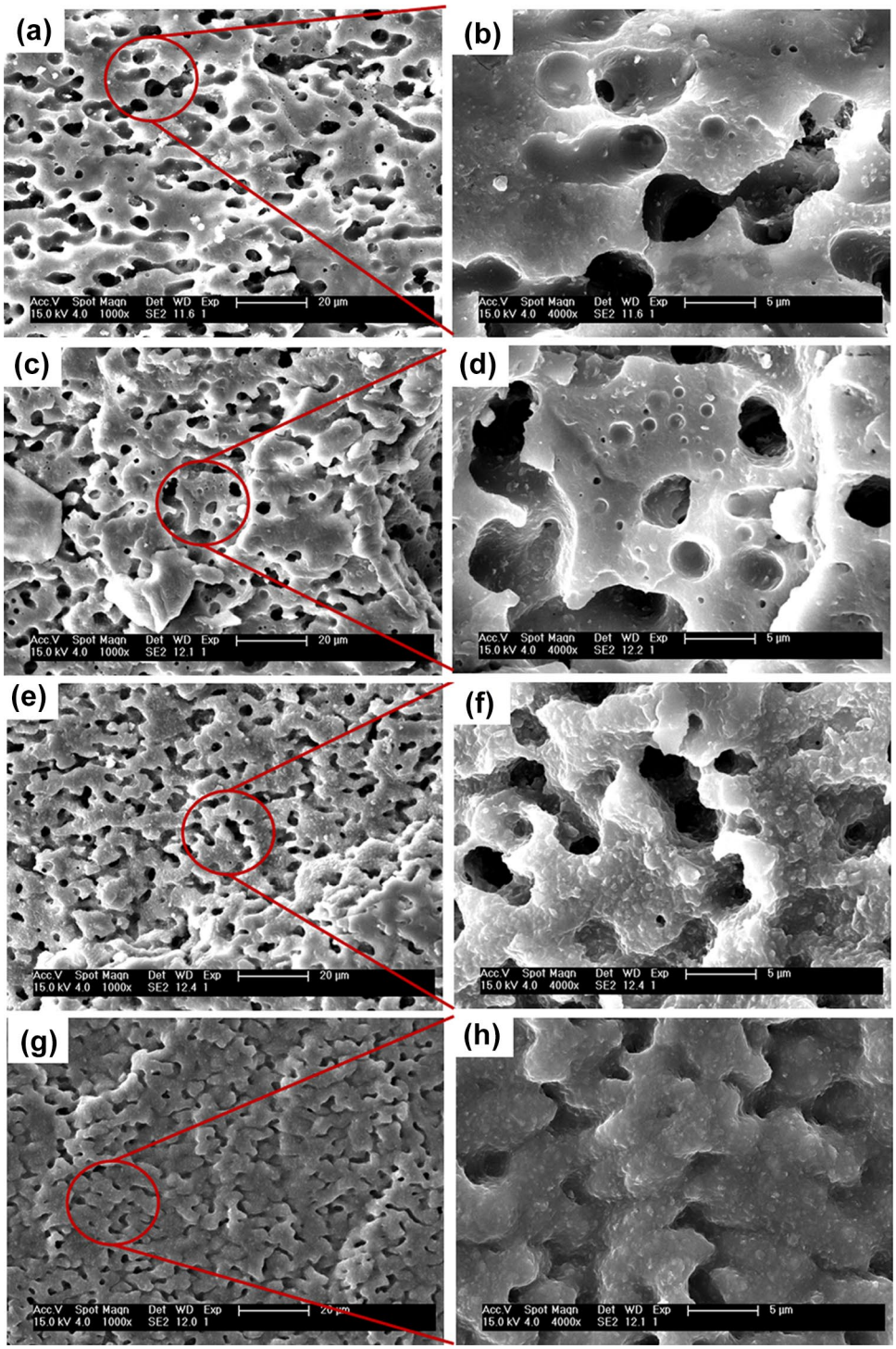

Fig. 1 SEM images of cryofractured surface of the PBS/PPC binary and PBS/PPC/PVAc ternary blends after etching in the acetone solution: **a**, **b** PBS/PPC, **c**, **d** PBS/PPC-5, **e f** PBS/PPC-10, and **g h** PBS/PPC-20

decrease in T_g of the components in immiscible blends has also been observed in other systems [28, 29]. The decrease in T_g of PBS matrix in the binary blend might be caused by the existence of phase interface between PBS matrix and PPC minor phase originated from the immiscibility between them [30]. In the immiscible blends, small molecules, short-chain, and long-chain ends of the components are enriched near the phase interface, which causes excess free volume at the interface, resulting in an enhanced chain mobility and a depression of T_g [31, 32]. Contrary to the change in T_g of PBS, T_g of PPC in the binary blend increased compared to neat PPC, which might be due to the reduction of the available free volume of PPC dispersed phase during the glass transition of PPC and PBS [33].

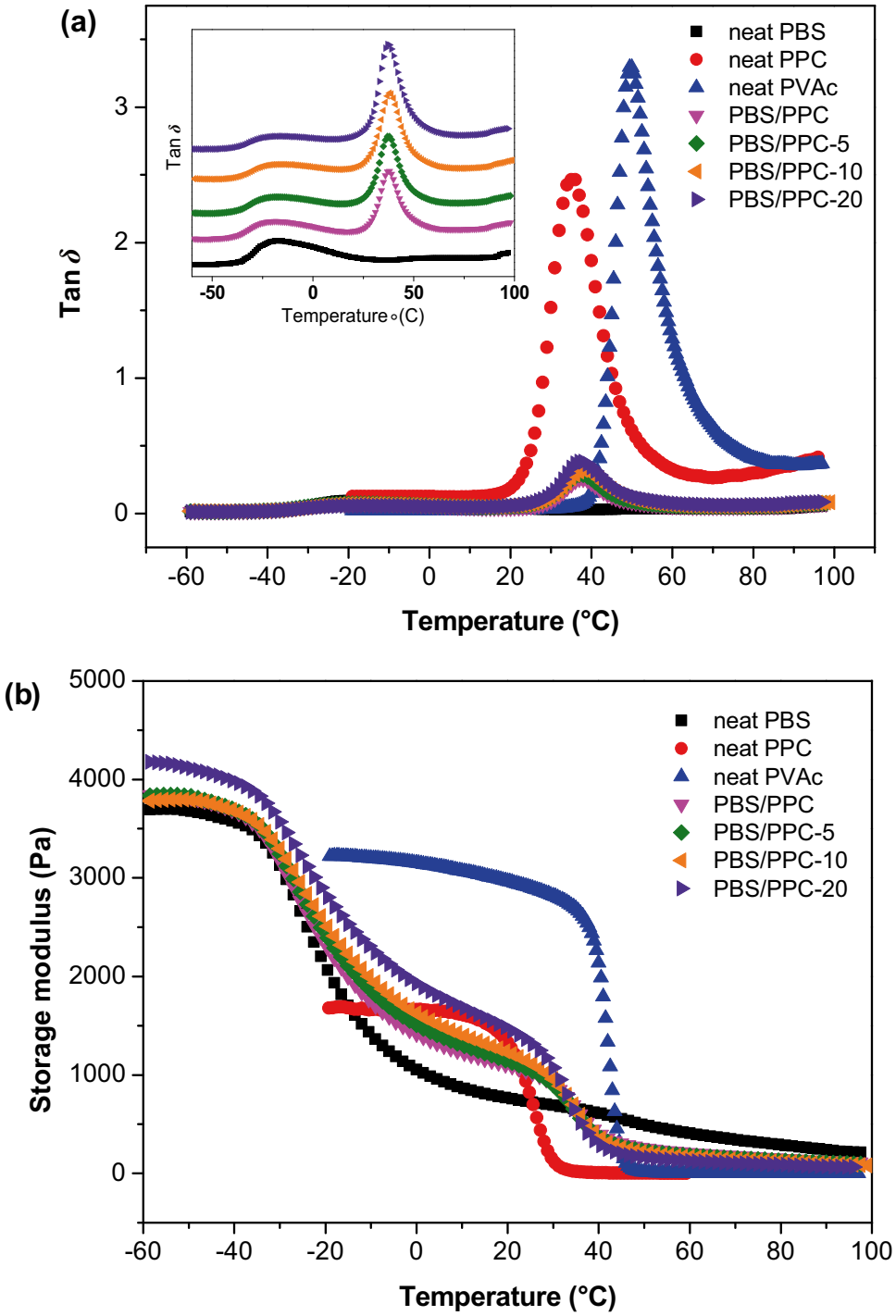

Fig. 2 Temperature dependence of **a** tan δ and **b** storage modulus (E') for neat components and the PBS/PPC binary and PBS/PPC/PVAc ternary blends

In the case of the PBS/PPC/PVAc ternary blends, there were two glass transitions on the tan δ curves. The T_g at about − 20.0 °C was corresponded to the PBS matrix, and that at about 37 °C was corresponded to the PPC phase. It was found that the T_g values of PPC hardly changed with the PVAc concentration varied, demonstrating that PVAc was immiscible with PPC in amorphous region. Moreover, the T_g values of PBS only increased by 1.9 °C, as the PVAc content increased to 20 wt%. Such a slight increase in T_g suggested that PVAc was partially miscible with PBS, and PVAc might be selectively dispersed at the interface, which was in good agreement with our previous research [25]. The glass transition peaks of PVAc were not observed on the tan δ curves, which may be attributed to the interference of the glass transition of PVAc by PPC due to the low concentration of PVAc in the ternary blends.

Table 1 Glass transition temperatures (T_g) from DMA test for all samples

Samples	neat PBS	neat PPC	neat PVAc	PBS/PPC	PBS/PPC-5	PBS/PPC-10	PBS/PPC-20
$T_{g,PBS}$ (°C)	−19.0	-	-	−20.8	−20.0	−19.4	−18.9
$T_{g,PPC}$ (°C)	-	34.5	-	37.8	37.3	38.1	37.3
$T_{g,PVAc}$ (°C)	-	-	48.5	-	-	-	-

It can be seen from Fig. 2b that the highest storage modulus of neat PBS was 3.7 GPa, and the storage modulus dropped sharply at about −30 °C because the glass transition began to occur. PPC and PVAc showed the highest storage modulus of 1.7 and 3.2 GPa, respectively, at temperature below their T_gs. When the glass transitions of PPC and PVAc happened at around 20 and 40 °C, the storage modulus of PPC and PVAc decreased sharply. As the temperature was lower than −30 °C, all the components of ternary blends were glassy, so the storage modulus of PBS/PPC/PVAc ternary blends was not greatly affected by the PVAc concentration. When the temperature was between −30 and 40 °C, that is, lower than the T_g of PVAc and higher than the T_g of PBS, the storage modulus of ternary blends with high PVAc content was higher. This was because elastic PBS matrix could be reinforced by glassy PVAc and PPC. When the temperature was higher than 50 °C, the storage modulus of PBS/PPC/PVAc ternary blend decreased as the content of PVAc increased. This can be attributed to both PVAc and PPC which were transformed into a highly elastic state and showed lower storage modulus compared with neat PBS.

Thermal and crystallization behaviors of the blends

Since PBS is a semi-crystalline polymer, its mechanical, rheological, and thermal properties depend to a large extent on its degree of crystallinity and solid-state morphology. Accordingly, it is of great significance to investigate the thermal and crystallization behaviors of ternary blends. Figure 3a shows DSC thermograms recorded from the cooling scan at a cooling rate of 10 °C min^{-1} for neat PBS and PBS/PPC binary and PBS/PPC/PVAc ternary blends. The detail results, including crystallization peak temperatures (T_c) and crystallization enthalpy (ΔH_c), are listed in Table 2.

It is well known that the T_c can be used to estimate the nucleation rate of non-isothermal melt crystallization, and a higher T_c indicates a faster nucleation rate [34]. As can be seen from Fig. 3a, neat PBS shows T_c at 75.1 °C, and T_c of PBS/PPC binary blend decreased to 73.4 °C. However, T_c of PBS/PPC/PVAc ternary blends were higher than that of neat PBS and increased to 80.0, 82.2, and 83.3 °C with PVAc concentration increased to 5 wt%, 10 wt%, and 20 wt%, respectively. In order to further study the influence of PPC and PVAc on the non-isothermal crystallization of PBS, Fig. 2b presents the relative crystallinity curves of all samples. Another important parameter of non-isothermal crystallization, the crystallization half-time ($t_{1/2}$), that is, the crystallization time required for the relative crystallinity to reach 50%, can be directly obtained from Fig. 2b and are also listed in Table 2. The value of $t_{1/2}$ for neat PBS was 1.08 min, while the $t_{1/2}$ of PBS in PBS/PPC binary blend was 1.16 min, suggesting that the crystallization of PBS was restricted by the presence of the PPC phase. This is probably caused by the phase separation of the PBS/PPC binary blend where amorphous PPC impeded the nucleation and crystalline growth of PBS. However, in the case of PBS/PPC/PVAc ternary blends, the $t_{1/2}$ values decreased with the increasing PVAc content, indicating that introduction of PVAc and PPC promoted nucleation and accelerated the crystallization rate of PBS matrix. The reason for the increase of the crystallization rate of PBS is that PVAc can serve as nucleating centers to accelerate PBS crystallization due to the partial miscibility between PBS and PVAc.

Figure 4 shows the second heating scan thermograms of neat PBS and its binary and ternary blends at a heating rate of 10 °C min^{-1}. The melting peak temperature (T_m) and melting enthalpy (ΔH_m) are also summarized in Table 2. As shown in Fig. 4, the T_m of neat PBS could be observed at 115.5 °C. The T_ms of PBS phase in the binary and ternary blends were about 1 °C lower than that of pure PBS, which was attributed to the presence of PVAc and PPC which affected the perfection of crystals and reduced the thickness of lamellae.

In addition, the degree of crystallinity (X_c) of neat PBS and its blends can also be used to analyze the influence of the presence of PPC and PVAc on the crystallization behavior of PBS. The X_c of neat PBS was 52.3%, and it increased to 56.6% in the case of the PBS/PPC binary blend. This may be because the addition of PPC reduced the crystallization rate of PBS, leading to better stacking and arrangement of PBS molecular chains, and the X_c increased instead. For the PBS/PPC/PVAc ternary blends, the X_c decreased with the increasing PVAc content. It was worth noting that the ternary blend containing 5 wt% PVAc had the highest X_c, which was higher than that of neat PBS. The PVAc phase acted as a heterogeneous crystal nucleus increased nucleation density and the crystallization rate. In the process of crystallization, a

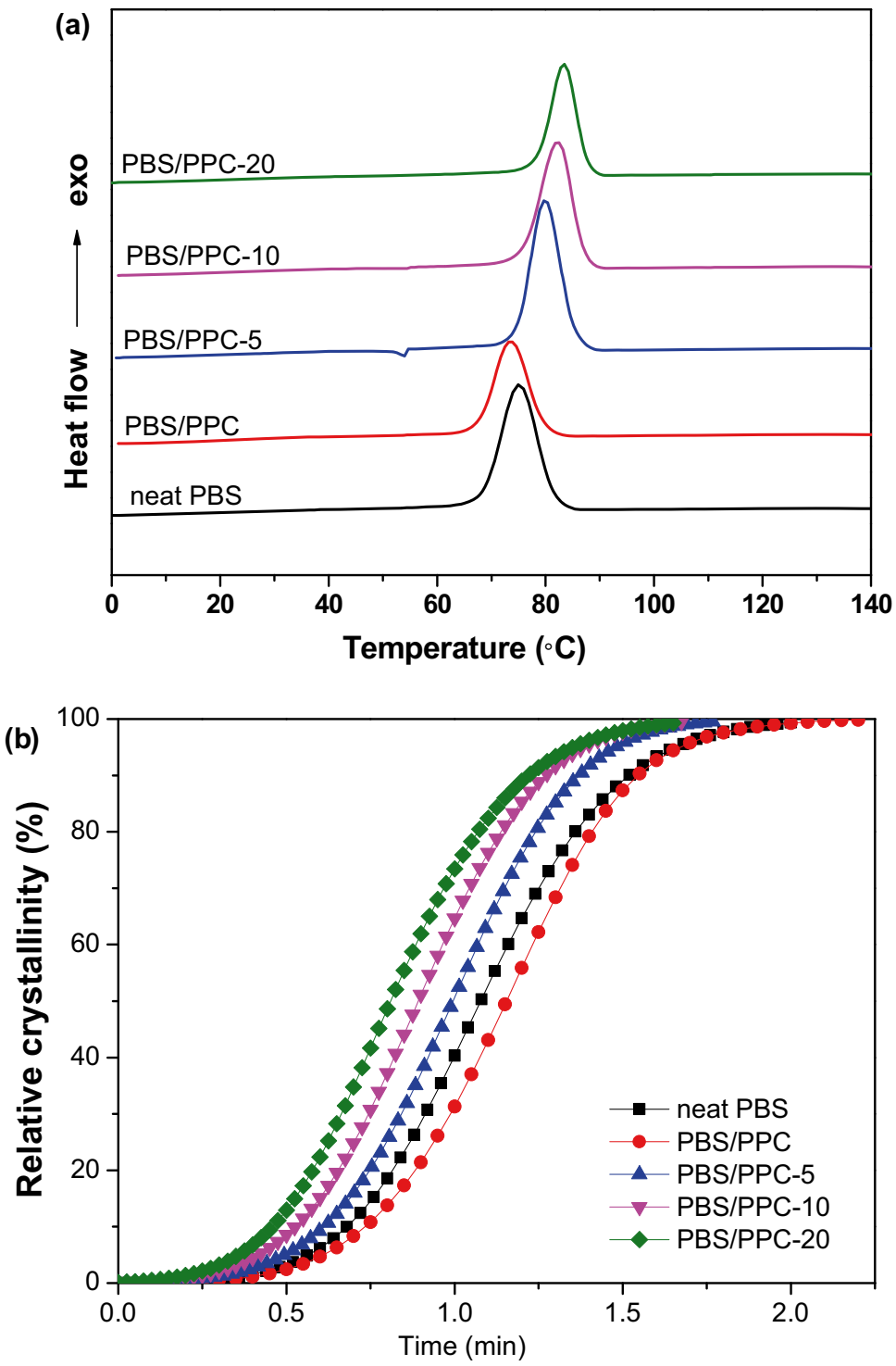

Fig. 3 **a** Cooling DSC thermograms of neat PBS and the PBS/PPC binary and PBS/PPC/PVAc ternary blends recorded at a cooling rate of 10 °C min^{-1}, and **b** relative crystallinity curves

large number of crystals generated by the high-density nucleation centers collided with each other due to space constraints, which limited the crystal growth and caused the X_c to decrease. In the case of PBS/PPC/PVAc ternary blend with a PVAc content of 5 wt%, nucleation and crystal growth of PBS reached a balance.

Table 2 Non-isothermal melt crystallization and melting parameters of neat PBS and the PBS/PPC binary and PBS/PPC/PVAc ternary blends

Sample	T_c (°C)	$t_{1/2}$ (min)	ΔH_c (J/g)	T_m (°C)	ΔH_m (J/g)	X_c (%)
neat PBS	75.1	1.08	58.5	115.5	57.7	52.3
PBS/PPC	73.4	1.16	59.3	114.4	62.4	56.6
PBS/PPC-5	80.0	0.99	63.0	114.8	65.1	59.0
PBS/PPC-10	82.3	0.89	59.3	114.2	59.1	53.6
PBS/PPC-20	83.3	0.81	59.2	114.6	56.6	51.3

ΔH_m and ΔH_c are corrected by the PBS content in the PBS/PPC binary and PBS/PPC/PVAc ternary blends

Rheological properties

It is well known that the rheological properties can provide a lot of useful information about morphological structure of multiphase polymeric blend system because of the sensitivity of rheological properties to the interfacial interactions between the components. To check the influence of PVAc and PPC minor phase on the rheological properties of PBS matrix, oscillatory shear rheological tests were performed at 150 °C. The dependence of the storage modulus (G'), loss modulus (G''), complex viscosity (|η*|), and damping factor (tan δ) on the angular frequency of neat PBS and PVAc as well as the PBS/PPC binary and PBS/PPC/PVAc ternary blends are presented in Fig. 5.

From Fig. 5a, the G' of neat PBS melt in the low frequency region showed a linear relationship with angular frequency, indicative of its liquid-like behavior. Neat PVAc exhibited higher G' than neat PBS over the entire angular frequency range on account of its high melt elasticity. Moreover, the G' of PBS/PPC binary was significantly higher than that of neat PBS. Especially at the frequency of 0.05 rad/s, G' of PBS/PPC binary blend increased more than 3 order of magnitude. This result suggested that the PPC phase enhanced the PBS melt. Furthermore, the introduction of PVAc into PBS/PPC blend from 5 to 20 wt % gradually raised the G' of ternary blend, implying that the PVAc phase also improved the melt elasticity of PBS, because neat PVAc had much higher melt elasticity and viscosity than neat PBS. In addition, the PBS/PPC binary and PBS/PPC/PVAc ternary blends represented less frequency dependence in the low frequencies, suggesting a solid-like behavior. This solid-like behavior may be attributed to the existence of a network structure and/or agglomerates of dispersed PVAc and PPC domains that were immiscible with PBS matrix [35]. According to Fig. 5b, PVAc showed a higher G'' than neat PBS in the low and intermediate frequencies, but had a lower G'' than neat PBS in the high frequencies, indicating that the dependence of G'' of PVAc on the angular frequency was not as obvious as PBS. Similar to the G', the incorporation of PVAc into PBS/PPC blend steadily increased the G'' of blends.

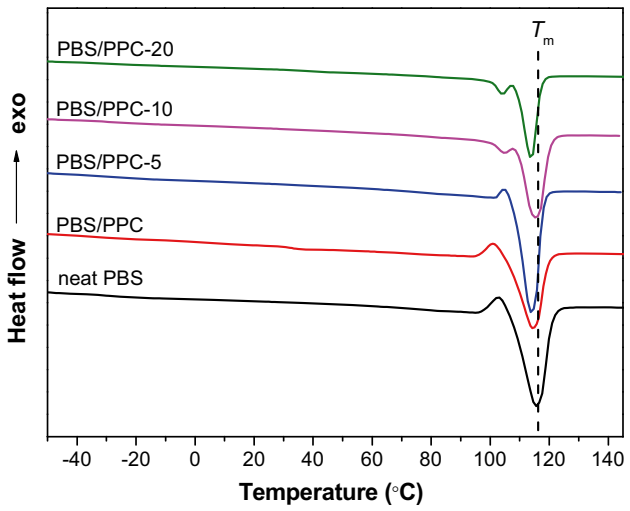

Fig. 4 Second heating DSC thermograms of neat PBS and the PBS/PPC binary and PBS/PPC/PVAc ternary blends at a heating rate of 10 °C min^{-1}

According to |η*| plots in Fig. 5c, neat PBS displayed a Newtonian behavior over the entire range of frequency, while neat PVAc exhibited an obvious shear thinning effect with respect to frequency. The viscosity of PVAc was significantly higher than that of PBS in the entire frequency range, and the viscosity difference between neat PBS and PVAc became more pronounced as the frequency decreased. The |η*| of blends was lower than neat PVAc and higher than neat PBS. For the PBS/PPC/PVAc ternary blends, as the PVAc content increased, the Newtonian plateau gradually became smaller and viscosity increased.

As shown in Fig. 5d, the loss tangent (tan $\delta = G''/G'$) is related to the dissipation under dynamic deformation. A larger tan δ represents the viscous behavior of the material, on the contrary, a lower tan δ indicates more elastic behavior. As the angular frequency increased, the tan δ value of neat PBS became smaller, which suggested the viscoelastic liquid behavior of PBS [36]. Neat PVAc had much lower tan δ compared with neat PBS over the entire frequency range ascribed to its high viscosity. In the case of blends, the tan δ values were lower than that of neat PBS and higher than

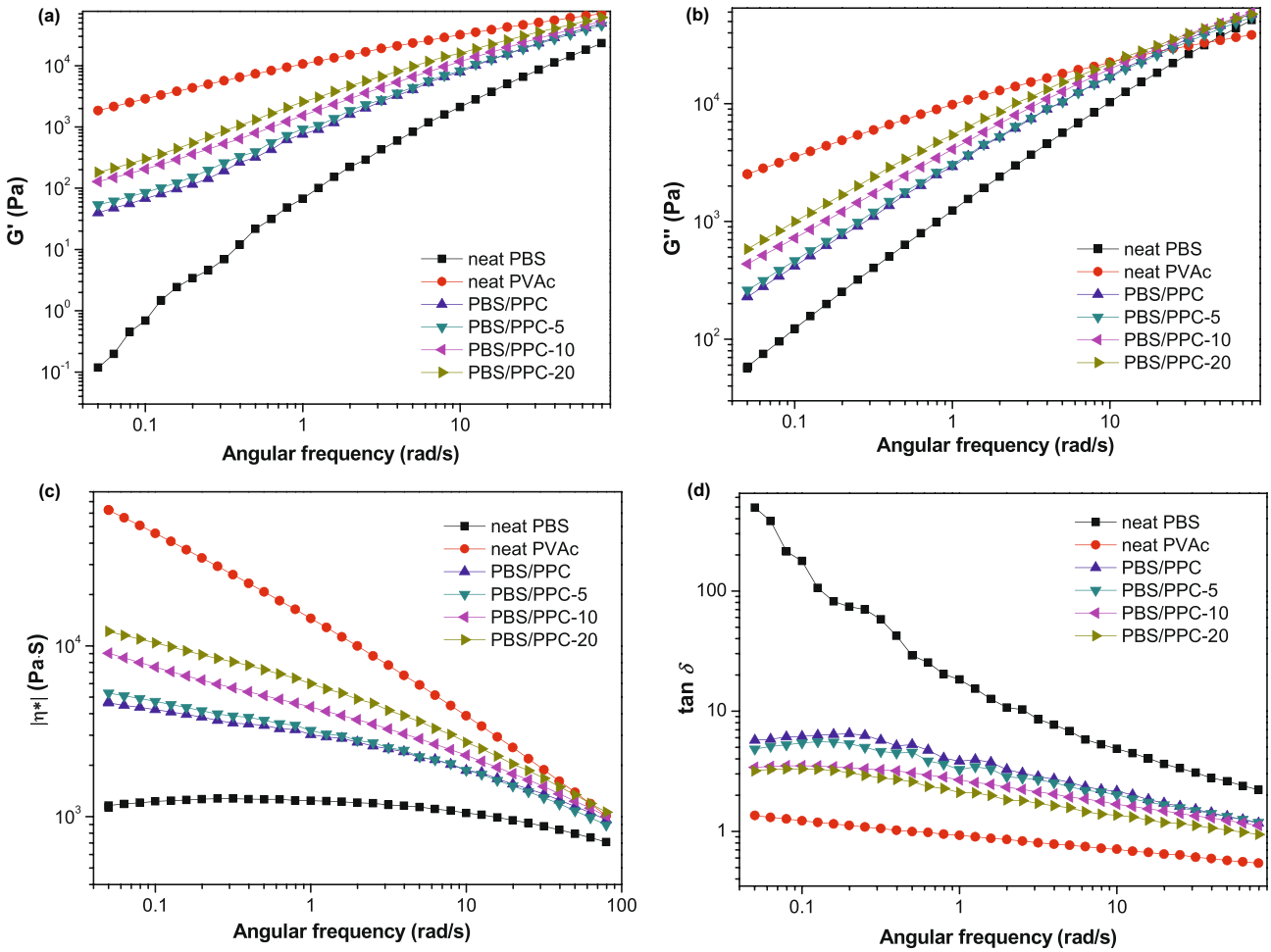

Fig. 5 **a** Storage modulus (G'), **b** loss modulus (G''), **c** complex viscosity ($|\eta^*|$), and **d** tan δ as a function of frequency for neat PBS, and the PBS/PPC binary and PBS/PPC/PVAc ternary blends at 150 °C

that of neat PVAc. Moreover, the PBS/PPC binary blend showed higher tan δ values than those of PBS/PPC/PVAc ternary blends. The data demonstrated that the tan δ of the ternary blends gradually reduced with the PVAc content. These observations were due to the lower damping of amorphous PVAc compared with semi-crystalline PBS.

The Cole–Cole plot can provide useful information about the structural changes and miscibility of the multiphase polymer systems [37]. For the PBS/PPC binary blend in this work, Cole – Cole plot (Fig. 6a) exhibited two semicircular arcs. The left and right side semicircular arcs were corresponded to the local dynamic relaxation and long-term restricted relaxation of PBS matrix, respectively, which again illustrated the immiscibility of PBS and PPC. Moreover, PBS/PPC/PVAc ternary blends showed a longer relaxation time with the increasing PVAc content, which was attributed to the physical interactions between PBS and PVAc due to their partial miscibility, and hindrance effect of high viscosity PVAc on the PBS chains.

The plot of log G' as a function of log G'' (Han plot) can be used to evaluate the miscibility of multiphase polymer blend [38]. The Han plots have the same slopes in the low modulus region, indicating that the components of the blends are miscible, otherwise they are immiscible. Figure 6b presents the Han plots of all samples at 150 °C. From Fig. 6b, the slopes of the Han plots of the blends in the low modulus region deviated from that of neat PBS, suggesting the immiscibility of PBS and PPC.

Tensile mechanical properties

The stress – strain curves of neat PBS and PBS/PPC binary and PBS/PPC/PVAc ternary blends with different PVAc concentrations are depicted in Fig. 7. The tensile properties, including breaking strength, elongation at break, yield strength, and Young's modulus obtained from Fig. 7 are listed in Table 3. Neat PBS was a soft polymer with a high tensile strain of 512% and Young's modulus of 507 MPa.

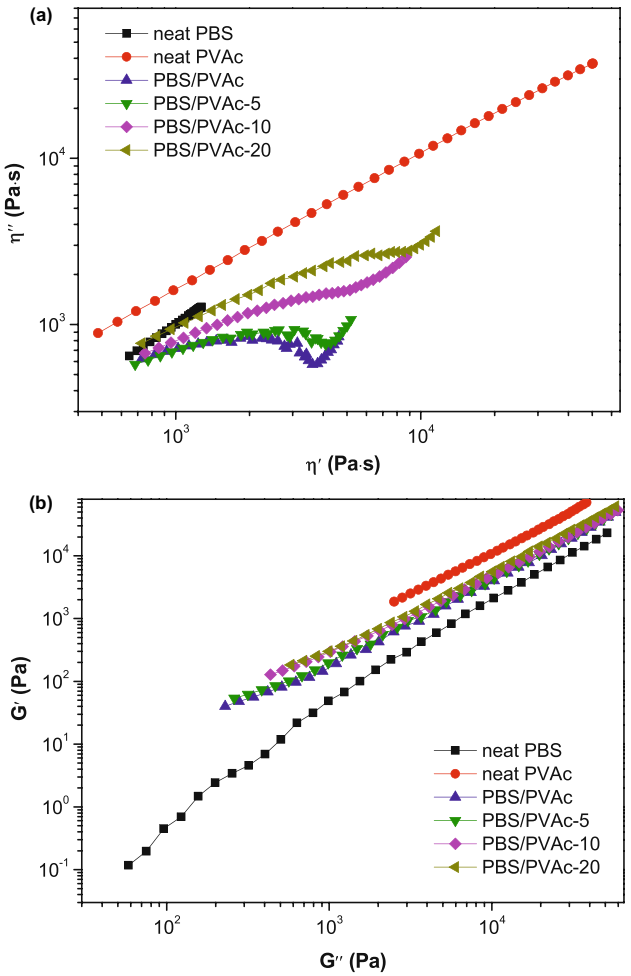

Fig. 6 **a** Cole–Cole and **b** Han curves of neat PBS, neat PVAc, and the PBS/PPC binary and PBS/PPC/PVAc ternary blends at 150 °C

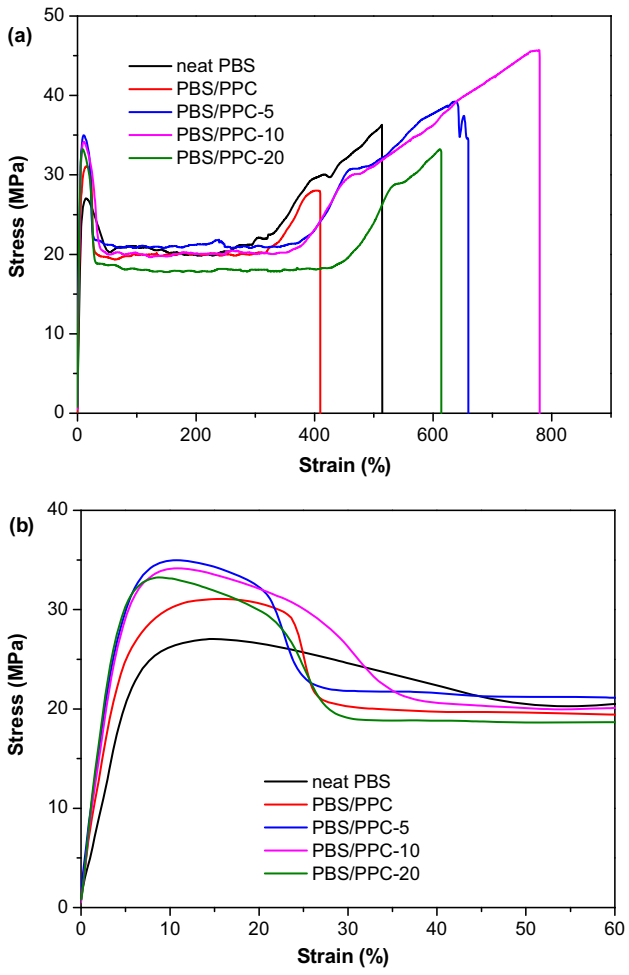

Fig. 7 **a** Tensile stress–strain curves of neat PBS and the PBS/PPC binary and PBS/PPC/PVAc ternary blends and **b** details of stress–strain curves at low strain

Although PBS had a high breaking strength of about 36 Mpa, its lower yield strength (≈27 Mpa) negatively affected the performance of PBS. Both binary and ternary blends exhibited ductile behavior, with a significant yield point and a stable necking process. As can be seen from Table 3, the PBS/PPC binary blend displayed improved Young's modulus of 697 MPa and yield strength of 31 MPa, whereas the breaking strength and elongation at break decreased to 30 MPa and 409%, respectively. This can be attributed to the introduction of stiff PPC into the PBS matrix.

Interestingly, the PBS/PPC/PVAc ternary blends showed a good balance of tensile mechanical properties compared with the binary blend and neat PBS. As the PVAc content increased from 5 to 20 wt%, the Young's modulus increased to 1239 MPa, which was 145% higher than neat PBS, and the breaking strength and elongation at break first increased and then decreased. Among them, a ternary blend with a PVAc content of 10 wt% showed the best tensile mechanical properties with Young's modulus of 981 MPa, elongation at break of 779%, yield strength of 34 MPa, and breaking strength of 46 MPa, which were increased by 93%, 52%, 26%, and 28% respectively, compared with neat PBS. There were two reasons for the simultaneous strengthening and toughening of the PBS/PPC/PVAc ternary blends. On the one hand, the decreasing degree of crystallinity of ternary blends with increasing PVAc content led to more amorphous region in the PBS matrix, which was easier to be oriented and strengthened during stretching [3]. On the other hand, the phase morphology also affected the mechanical properties of the PBS/PPC/PVAc ternary blends. The addition of PVAc refined the dispersed phase of the ternary blends, leading to the improvement of mechanical properties. When the PVAc content increased to 10 wt%, the phase morphology of the ternary blends evolved from sea-island dispersion based on PBS matrix to co-continuous structure. As a result, the mechanical properties further increased. As

Table 3 Tensile properties of neat PBS and the PBS/PPC binary and PBS/PPC/PVAc ternary blends

Sample	Young's modulus (MPa)	Yield strength (MPa)	Breaking strength (MPa)	Elongation at break (%)
neat PBS	507 ± 23	27.0 ± 1.7	36.3 ± 1.5	512 ± 36
PBS/PPC	697 ± 31	31.1 ± 1.5	30.0 ± 1.9	409 ± 22
PBS/PPC-5	810 ± 39	35.0 ± 2.0	39.2 ± 0.8	657 ± 41
PBS/PPC-10	981 ± 41	34.2 ± 1.8	45.7 ± 2.9	779 ± 53
PBS/PPC-20	1239 ± 45	33.0 ± 1.2	33.2 ± 2.1	623 ± 40

the PVAc content increased to 20 wt%, the tensile strength and elongation at break decreased due to the coarsening of the co-continuous phase morphology. Only the tensile modulus sensitive to the co-continuous structure continued to increase to 1239 MPa, which was because of the synergistic effect of the tensile modulus of the two phases [39].

Consequently, the excellent mechanical properties of PBS/PPC/PVAc ternary blends were ascribed to the combined effect of the degree of crystallinity of the PBS matrix and phase morphology of ternary blends. This combination of high flexibility and stiffness, which cannot be prepared by traditional polymer binary blends, will broaden the application fields and scope of biodegradable polymers.

Conclusions

In the present work, the biodegradable PBS/PPC/PVAc ternary blends at different PVAc contents were initially prepared via melt blending for the purpose of obtaining excellent mechanical properties. SEM observations showed that the introduction of PVAc into PBS/PPC binary blend refined the phase morphology. With the increase of PVAc content, the phase morphology of the ternary blends developed from a sea-island structure to a co-continuous structure. The DMA studies indicated that PBS and PPC were immiscible, and PVAc displayed partially miscible with PBS and immiscible with PPC. Moreover, the thermal and non-isothermal crystallization behaviors results suggested that the crystallization of PBS was inhibited by the presence of PPC, whereas the introduction of PVAc and PPC promoted the crystallization of PBS matrix. The rheological properties of PBS, including storage modulus, loss modulus, and complex viscosity were increased by the addition of PPC and PVAc. Intriguingly, the combination of improved tensile strength, modulus, and ductility was obtained for the PBS/PPC/PVAc ternary blends due to the formation of the co-continuous phase morphology.

This work is supported by the Chinese Academy of science and technology service network planning (KFJ-STS-QYZD-140), a program of Cooperation of Hubei Province and Chinese Academy of Sciences.

Funding This work is supported by the Chinese Academy of Science and Technology Service Network Planning (KFJ-STS-QYZD-140), a program of Cooperation of Hubei Province and Chinese Academy of Sciences.

Declarations

Conflict of interest The authors declare no competing interests.

References

1. Li Y, Zhao L, Han C, Yu Y (2020) Biodegradable blends of poly(butylene adipate-co-terephthalate) and stereocomplex polylactide with enhanced rheological, mechanical properties and thermal resistance. Colloid Polym Sci 298:463–475
2. Wang P, Tian Y, Wang G, Xu Y, Yang B, Lu B, Zhang W, Ji J (2015) Surface interaction induced transcrystallization in biodegradable poly(butylene succinate)-fibre composites. Colloid Polym Sci 293:2701–2707
3. Du X, Wang Y, Huang W, Yang J, Wang Y (2015) Rheology and non-isothermal crystallization behaviors of poly(butylene succinate)/graphene oxide composites. Colloid Polym Sci 293:389–400
4. Santagata G, Valerio F, Cimmino A, Poggetto GD, Masi M, Biase MD, Malinconico M, Lavermicocca P, Evidente A (2017) Chemico-physical and antifungal properties of poly(butylene succinate)/cavoxin blend: study of a novel bioactive polymeric based system. Eur Polym J 94:230–247
5. Xu J, Guo BH (2010) Poly (butylene succinate) and its copolymers: research, development and industrialization. Biotechnol J 5:1149–1163
6. Liang Z, Pan P, Zhu B, Dong T, Inoue Y (2010) Mechanical and thermal properties of poly(butylene succinate)/plant fiber biodegradable composite. J Appl Polym Sci 115:3559–3567
7. Langanke J, Wolf A, Hofmann J, Bohm K, Subhani MA, Müller TE, Leitner W, Gürtler C (2014) Carbon dioxide (CO_2) as sustainable feedstock for polyurethane production. Green Chem 16:1865–1870
8. Muthuraj R, Mekonnen T (2018) Recent progress in carbon dioxide (CO_2) as feedstock for sustainable materials development: co-polymers and polymer blends. Polymer 145:348–373

9. Wu D, Yuan L, Laredo E, Zhang M, Zhou W (2012) Interfacial properties, viscoelasticity, and thermal behaviors of poly(butylene succinate)/polylactide blend. Ind Eng Chem Res 51:2290–2298
10. Deng Y, Thomas NL (2015) Blending poly(butylene succinate) with poly(lactic acid): ductility and phase inversion effects. Eur Polym J 71:534–546
11. Monika MN, Katiyar V (2019) Generalized kinetics for thermal degradation and melt rheology for poly (lactic acid)/poly (butylene succinate)/functionalized chitosan based reactive nanobiocomposite. Int J Biol Macromol 141:831–842
12. Chen S, Ma C, Zhang G (2016) Biodegradable polymers for marine antibiofouling: poly(ε-caprolactone)/poly(butylene succinate) blend as controlled release system of organic antifoulant. Polymer 90:215–221
13. Qiu Z, Komura M, Ikehara T, Nish T (2003) Miscibility and crystallization behavior of biodegradable blends of two aliphatic polyesters. Poly(butylene succinate) and poly(ε-caprolactone). Polymer 44:7749–7756
14. Hexig B, Alata H, Asakawa N, Inoue Y (2021) Novel biodegradable poly(butylene succinate)/poly(ethylene oxide) blend film with compositional and spherulite-size gradients. J Polym Sci Pol Phys 43:368–377
15. Qiu Z, Ikehara T, Nishi T (2003) Miscibility and crystallization in crystalline-crystalline blends of poly(butylene succinate)/poly-(ethylene oxide). Polymer 44:2799–2806
16. Qiu Z, Ikehara T, Nishi T (2003) Poly(hydroxybutyrate)/poly(butylene succinate) blends: miscibility and nonisothermal crystallization. Polymer 44:2503–2508
17. Qiu Z, Yang W (2006) Crystallization kinetics and morphology of poly(butylene succinate)/poly(vinyl phenol) blend. Polymer 47:6429–6437
18. Zhang H, Sun X, Chen Q, Ren M, Zhang Z, Zhang H, Mo Z (2007) Miscibility, crystallization and mechanical properties of PPC/PBS blends. Chinese J Polym Sci 25:589–597
19. Pang M, Qiao J, Jiao J, Wang S, Xiao M, Meng Y (2008) Miscibility and properties of completely biodegradable blends of poly(propylene carbonate) and poly(butylene succinate). J Appl Polym Sci 107:2854–2860
20. Calderón BA, McCaughey MS, Thompson CW, Sobkowicz MJ (2019) Blends of renewable poly(butylene succinate) and poly(propylene carbonate) compatibilized with maleic anhydride using quad screw reactive extrusion. Ind Eng Chem Res 58:487–495
21. Li Y, Lei Y, Yao S, Han C, Yu Y, Xiao L (2020) Miscibility, crystallization, rheological and mechanical properties of biodegradable poly(3-hydroxybutyrate-*co*-4-hydroxybutyrate)/poly(vinyl acetate) blends. Thermochim Acta 693:178755
22. Huang T, Yang J, Zhang N, Zhang J, Wang Y (2018) Crystallization of poly(L-lactide) in the miscible poly(L-lactide)/poly(vinyl acetate) blend induced by carbon nanotubes. Polym Bull 75:2641–2655
23. Sivalingam G, Karthik R, Madras G (2004) Blends of poly(ε-caprolactone) and poly(vinyl acetate): mechanical properties and thermal degradation. Polym Degrad Stabil 84:345–351
24. Shafee EE (2001) Investigation of the phase structure of poly(3-hydroxybutyrate)/poly(vinyl acetate) blends by dielectric relaxation spectroscopy. Eur Polym J 37:451–458
25. Li Y, Han C, Xiao L, Yu Y, Zhou G, Xu M (2021) Miscibility, morphology, and properties of poly(butylene succinate)/poly(vinyl acetate) blends. Colloid Polym Sci 299:105–116
26. Shi K, Liu Y, Hu X, Su T, Li P, Wang Z (2018) Preparation, characterization, and biodegradation of poly(butylene succinate)/cellulose triacetate blends. Int J Biol Macromol 114:373–380
27. Sundararaj U, Macosko CW (1995) Drop breakup and coalescence in polymer blends: the effects of concentration and compatibilization. Macromolecules 28:2647–2657
28. Han L, Han C, Zhang H, Chen S, Dong L (2012) Morphology and properties of biodegradable and biosourced polylactide blends with poly(3-hydroxybutyrate-*co*-4-hydroxybutyrate). Polym Composite 33:850–859
29. Shibata M, Teramoto N, Inoue Y (2007) Mechanical properties, morphologies, and crystallization behavior of plasticized poly(L-lactide)/poly(butylene succinate-co-L-lactate) blends. Polymer 48:2768–2777
30. Kumar M, Mohanty S, Nayak SK, Parvaiz MR (2010) Effect of glycidyl methacrylate (GMA) on the thermal, mechanical and morphological property of biodegradable PLA/PBAT blend and its nanocomposites. Bioresour Technol 101:8406–8415
31. Sakai F, Nishikawa K, Inoue Y, Yazawa K (2009) Nucleation enhancement effect in poly(L-lactide) (PLLA)/poly(ε-caprolactone) (PCL) blend induced by locally activated chain mobility resulting from limited miscibility. Macromolecules 42:8335–8342
32. Kajiyama T, Tanaka K, Takahara A (1997) Surface molecular motion of the monodisperse polystyrene films. Macromolecules 30:280–285
33. Thirtha V, Lehman R, Nosker T (2006) Morphological effects on glass transition behavior in selected immiscible blends of amorphous and semicrystalline polymers. Polymer 47:5392–5401
34. Wei X, Bao R, Cao Z, Zhang L, Liu Z, Yang W, Xue B, Yang M (2014) Greatly accelerated crystallization of poly(lactic acid): cooperative effect of stereocomplex crystallites and polyethylene glycol. Colloid Polym Sci 92:163–172
35. Mazidi MM, Edalat A, Berahman R, Hosseini FS (2018) Highly-toughened polylactide-(PLA-) based ternary blends with significantly enhanced glass transition and melt strength: tailoring the interfacial interactions, phase morphology, and performance. Macromolecules 51:4298–4314
36. Tian J, Yu W, Zhou C (2006) The preparation and rheology characterization of long chain branching polypropylene. Polymer 47:7962–7969
37. Hao X, Kaschta J, Liu X, Pan Y, Schubert DW (2015) Entanglement network formed in miscible PLA/PMMA blends and its role in rheological and thermo-mechanical properties of the blends. Polymer 80:38–45
38. Han CD, Kim J, Kim JK (1989) Determination of the order-disorder transition temperature of block copolymers. Macromolecules 22:383–394
39. Veenstra H, Verkooijen PCJ, van Lent BJJ, van Dam J, de Boer AP, Nijhof APHJ (2000) On the mechanical properties of co-continuous polymer blends: experimental and modeling. Polymer 41:1817–1826